Preliminary Analysis on Impact of Control-Rod Absorber Material Modeling on Severe Accident Progression and Fission-Product Release

Jungbin Yoon, Yoonhee Lee *
Dept. of Energy Engineering, Korea Institute of Energy Technology (KENTECH),
21 Kentech-gil, Naju-si, Jeonnam-Gwangju, 58330 Republic of Korea
**Corresponding author: yooney@kentech.ac.kr*

***Keywords :** Small Modular Reactor, Control rod, Source term, Severe accident, MELCOR

1. Introduction

Control-rod behavior can influence severe-accident progression through material-specific interactions and oxidation behavior. During core degradation, absorber materials can interact with surrounding core structures and, depending on the material, undergo additional reactions that affect the thermal and chemical conditions within the core. In particular, B_4C can react with steam after exposure from the control-rod sheath, generating additional heat and hydrogen during core degradation. Consequently, the representation of control-rod absorber materials can influence core degradation, hydrogen generation, and subsequent fission-product behavior during a severe accident.

The i-SMR, a South Korean pressurized-water small modular reactor (SMR), employs both Ag-In-Cd (AIC) and B_4C absorber materials within a single reactor core [1]. However, the current MELCOR core model does not allow multiple control-rod absorber materials to be represented simultaneously within a single core. [2] Consequently, severe-accident analyses of a mixed-absorber core require the absorber configuration to be simplified using a single-material representation, and the influence of this modeling choice on the predicted accident progression and fission-product behavior has not yet been clarified.

This study therefore evaluates the sensitivity of severe-accident predictions to the control-rod absorber representation by comparing AIC-only and B_4C-only core models under an identical accident scenario. The comparison focuses on core degradation, hydrogen generation, and fission-product release and distribution.

2. Methods

2.1 Configuration of the Base Reactor Model

The reactor model consists of a reactor vessel (RV) and a containment vessel (CV), with the CV subdivided into upper (UCV) and lower (LCV) compartments. The model also includes passive safety systems, including the Passive Emergency Core Cooling System (PECCS), Passive Containment Cooling System (PCCS), and Passive Auxiliary Feedwater System (PAFS) [3]. The core is discretized into seven radial rings and 16 axial levels, with fuel-loaded region representing the active core. The failure-temperature criteria for the core structures are modified using MELCOR sensitivity coefficients. The fuel-rod failure temperature for an unoxidized cladding thickness below 0.1 mm is set to 2,479 K, while the temperature criterion applicable regardless of the cladding condition is set to 2,800 K to represent the UO_2 melting temperature. The failure temperature for stainless-steel structures was set to 1,673 K. The reactor is assumed to be at end of equilibrium fuel cycle [1], and the initial fission-product inventory is calculated using ORIGEN. The MELCOR nodalization of the base reactor model is shown in Fig. 1.

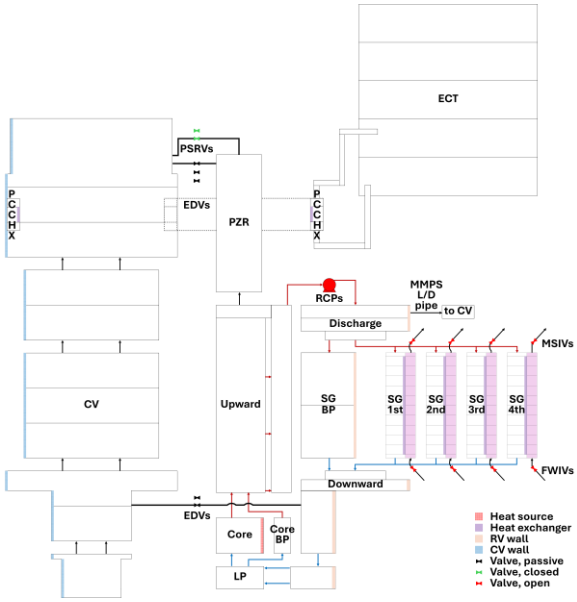


Fig. 1. MELCOR nodalization of the base reactor model.

2.2 Configuration of Control-Rod Models

The i-SMR employs two types of control rods with two different absorber materials, Ag-In-Cd (AIC) and B_4C, within a single core. [1] However, the current MELCOR core model does not allow multiple control-rod absorber materials to be represented simultaneously within a single core. [2] Therefore, a sensitivity analysis was performed using two separate core representations, in which the control-rod absorber material is modeled as either AIC or B_4C. The same base reactor model and accident conditions are applied to both cases.

B_4C can affect core degradation through its reaction with steam when exposed following failure of stainless-steel sheath. Accordingly, the B_4C model employs the B_4C control-rod oxidation model implemented in the MELCOR COR package. In this model, B_4C oxidation begins at 1,500 K, corresponding to the onset of eutectic interaction between B_4C and the stainless-steel. An effective eutectic liquefaction temperature of 1,700 K is used to represent gross slumping and relocation of the control rod absorber materials [4].

The two cases are hereafter referred to as the AIC and B_4C models, respectively. For each case, the absorber mass and oxidation-model settings are specified according to the selected control-rod material. The model parameters that differ between the two cases are summarized in Table I, while the remaining core-model parameters are maintained identically. Mass values vary with absorber density for the same volume across 53 banks, each with 24 control rods.

Table I: Identical MELCOR input of AIC and B4C cases.

Parameter	AIC	B4C
Material	Ag-In-Cd	B_4C
Absorber density	10.17 kg/m^3	2.52 kg/m^3
Absorber mass	1,829.1 kg	453.2 kg
Absorber oxidation	N/A	On

2.3 Accident Scenario and Analysis Conditions

For the sensitivity analysis, a 2-inch Loss of Coolant Accident (LOCA) through the Modular Makeup and Purification System letdown line inside the containment vessel (in-CV MMPS L/D LOCA) is selected as the initiating event. The Emergency Recirculation Valve (ERV) and PAFS are assumed to be unavailable to allow the accident to progress to severe core degradation. The containment vessel is assumed to remain isolated from the environment throughout the calculation, such that no environmental release of fission products is considered and the initial fission-product inventory remains within the modeled RV–CV system. Because the MMPS L/D line is located in the upper part of the reactor system, the selected scenario provides sufficient time for control-rod absorber material oxidation to develop, allowing its influence on severe accident progression to be evaluated.

3. Results

Fig. 2 shows the reactor vessel water level and the timing of core support plate failure for the AIC and B4C cases. The accident was initiated by the in-CV MMPS L/D LOCA at 0 s, resulting in a decrease in the reactor vessel coolant inventory and pressure. The reactor is tripped at 55.2 s by a high containment pressure signal, and core uncovery begins at approximately 23,200 s. As summarized in Table II, the early accident progression is similar between the two cases, with core uncovery and oxidation beginning at approximately 23,000 and 25,000 s, respectively. Noticeable differences between the AIC and B4C cases subsequently emerge during core degradation. The corresponding changes in the core-material mass fractions are provided in Fig. 3.

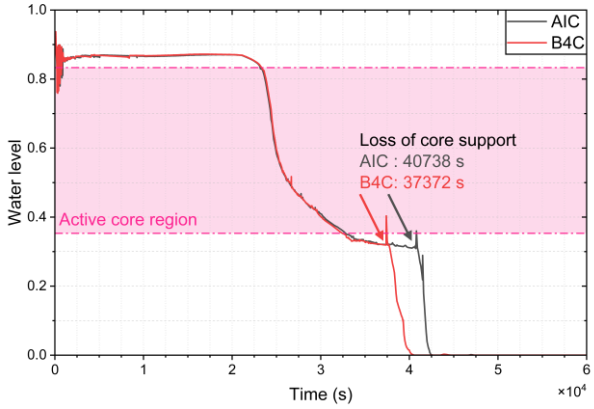


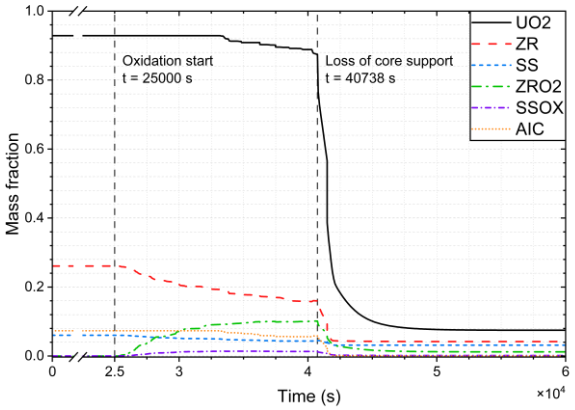
Fig. 2. Water level of core measured from RV bottom.

Table II. Accident chronicle of AIC and B4C models.

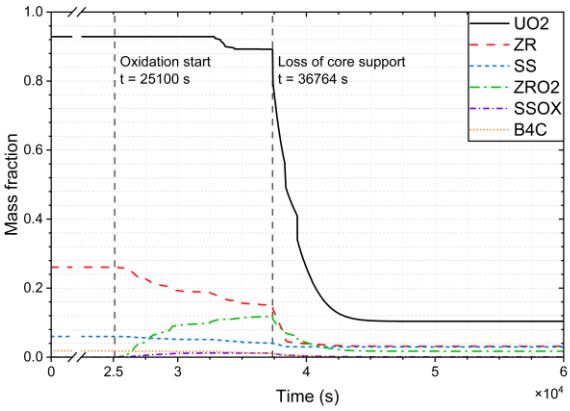
Event	AIC (s)	B4C (s)
Core top reveal	23,200	23,400
Oxidation start	25,000	25,100
CET > 923 K	25,413	25,867
Active core dryout	33,000	33,100
Loss of core support	40,738	37,372
Lower plenum dryout	42,700	40,600

The difference in accident progression becomes pronounced at the core support plate failure. The B4C case reached core support plate failure at 37,372 s, 3,366 s earlier than the AIC case at 40,738 s.

Following core uncovery, oxidation of the exposed core materials progresses in both cases. As shown in Fig. 3, the initial inventories of the major core materials are identical between the two cases, except for the control-rod absorber materials. The B4C case exhibits greater cumulative oxidation energy and hydrogen generation, as shown in Fig. 4. Prior to core support plate failure, the cumulative hydrogen generation reached 103.6 kg in the AIC case and 124.9 kg in the B4C case. In the B4C case, approximately 9.9% of the initial B_4C mass was consumed by the steam oxidation reaction. The additional oxidation associated with B_4C therefore contributed to the accelerated core degradation and earlier loss of core support observed in the B4C case.



(a) AIC



(b) B4C

Fig. 3. Core-Mass fraction of core materials in the upper core region.

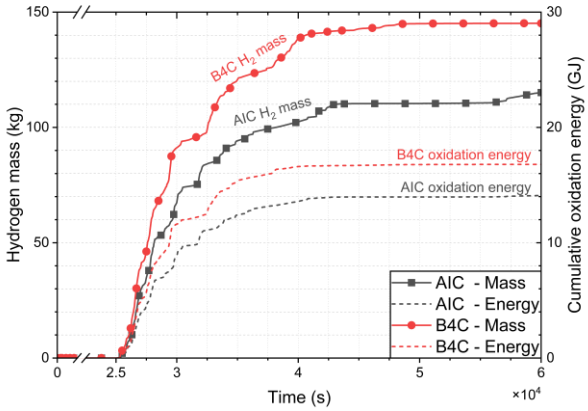


Fig. 4. Cumulative hydrogen and oxidation energy during the accident.

The influence of control-rod absorber modeling on fission-product release is evaluated using the release fractions predicted for each MELCOR class. The sensitivity of the predicted release fraction to the absorber representation varies among the MELCOR classes. Several classes, including Xe, Cs, I, Te, Ru, Ce, and La, show relatively similar release behavior between the two cases, whereas more noticeable differences are observed for Ba, Mo, Cd, and Ag.

Fig. 5 compares the release-fraction histories of Cs and AG as representative classes showing low and high sensitivity, respectively, to the absorber representation. For an event-based comparison, the release fractions of Cs and Ag are evaluated at active core dryout (CDO), loss of core support (LOS), and the end of analysis (EOA), as summarized in Table III. The release fraction at each event is evaluated at the corresponding event time for each case. The Cs release fractions differ by no more than 0.8 percentage points between the two cases at the selected accident events. In contrast, the Ag release fractions differ by 8.4, 11.2, and 7.9 percentage points at CDO, LOS, and EOA, respectively. Notably, the B4C case shows a higher Ag release fraction at CDO but lower fractions at LOS and EOA, indicating that the absorber representation affects not only the final release fraction but also the temporal evolution of Ag release.

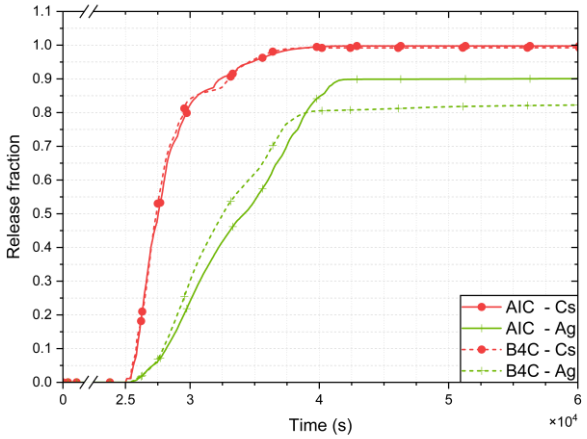


Fig. 5. Comparison of Cs and Ag release fractions for the AIC and B4C cases.

Table III. Cs and Ag release fractions at selected accident events*.

Class	AIC (%)			B4C (%)		
	CDO	LOS	EOA	CDO	LOS	EOA
Cs	91.2	99.7	99.8	90.5	98.9	99.3
Ag	45.1	87.6	90.1	53.5	76.4	82.2

* The release fraction for each event was evaluated at the corresponding event time of each case.

The fission-product distributions within the containment vessel at the end of the calculation (60,000 s) are summarized in Table IV. Because the containment vessel is isolated from the environment in both cases, no environmental release is considered, allowing the differences in fission-product transfer and distribution within the modeled RV–CV system to be compared directly.

The effect of absorber representation on the predicted CV inventory was also dependent on the MELCOR class. For example, the LCV fractions of Cs and Te were lower in the B4C case than in the AIC case, whereas the differences for several other classes are relatively small. Unlike most other classes, Xe showed larger fractions in the UCV than in the LCV in both cases.

Table IV. Fission-product distribution in the CV at 60,000 s.

Class	AIC (%)		B4C (%)	
	LCV	UCV	LCV	UCV
Xe	30.19	65.66	31.25	64.39
Cs	31.63	0.069	25.46	0.331
Ba	2.186	0.006	1.880	0.003
I	34.00	0.067	29.00	0.048
Te	17.16	0.201	12.46	0.122
Ru	0.234	0.001	0.196	0.001
Mo	5.573	0.0001	5.259	0.0002
Ce	0.015	0.00001	0.013	0.00001
La	0.015	0.00001	0.013	0.00001
Cd	5.259	0.014	5.477	0.005
Ag	3.652	0.002	3.747	0.001

* The integrity of the reactor vessel was maintained at 60,000 s.

4. Conclusions

This study evaluated the influence of control-rod absorber representation on severe-accident progression and fission-product behavior using MELCOR simulations of an in-CV MMPS L/D LOCA. The early accident progression was similar between the AIC and B4C cases; however, noticeable differences emerged following the onset of core degradation. The B4C case exhibited greater cumulative oxidation energy and hydrogen generation, with core support plate failure occurring 3,366 s earlier than in the AIC case. Prior to core support plate failure, cumulative hydrogen generation reached 103.6 kg and 124.9 kg in the AIC and B4C cases, respectively.

The influence of absorber representation also propagated to the predicted fission-product behavior, although the magnitude of the effect varied among the MELCOR classes. While several classes showed similar release behavior between the two cases, more noticeable differences were observed for selected classes, indicating that the sensitivity of fission-product release to absorber representation is class-dependent.

These results demonstrate that the selection of a single-material absorber representation can influence coupled severe-accident predictions from core degradation and hydrogen generation to fission-product behavior. For reactor designs employing multiple absorber materials within a single core, the inability to represent the actual mixed-absorber configuration should therefore be recognized as a modeling limitation when interpreting severe-accident analysis results.

ACKNOWLEDGEMENTS

This study was supported by the Nuclear Safety Research Program through the Regulatory Research Management Agency for SMRs (RMAS) and the Nuclear Safety and Security Commission (NSSC) of the Republic of Korea. (No. RS-2025-02311309).

REFERENCES

[1] Jin Sun Kim et al., “Reactor core design with enriched gadolinia burnable absorbers for soluble Boron-Free operation in the innovative SMR,” *Nuclear Engineering and Design*, vol 428, 2024.

[2] L.I. Albright et al., MELCOR Computer Code Manuals, Vol. 1: Primer and Users’ Guide, Version 2026.0, SAND2026-18477 O, 2026.

[3] Sang Gyu Lim et al., “Design characteristics of nuclear steam supply system and passive safety system for Innovative Small Modular Reactor (i-SMR),” *Nuclear Engineering and Technology*, vol 57, 2025.

[4] L.I. Albright et al., MELCOR Computer Code Manuals, Vol. 2: Reference Manual, Version 2026.0, SAND2026-18478 O, 2026.